Journal of Catalysis **192,** 77–87 (2000)
doi:10.1006/jcat.2000.2817, available online at http://www.idealibrary.com on IDEAL®

New Insights into Alkali-Catalyzed Gasification Reactions of Carbon: Comparison of N_2O Reduction with Carbon over Na and K Catalysts

Z. H. Zhu,* G. Q. Lu,*,[1] and R. T. Yang†

*Department of Chemical Engineering, The University of Queensland, Queensland 4072, Australia; and †Department of Chemical Engineering, University of Michigan, Ann Arbor, Michigan 48109-2136

Received September 1, 1999; revised January 11, 2000; accepted January 11, 2000

Catalytic conversion of N_2O to N_2 over Na- and K-impregnated activated carbon (Na/AC and K/AC) was investigated. K and Na are two representative and most active catalysts for the C–NO_x reactions. Carbon samples with different K and Na loadings were characterized by N_2 adsorption, thermal decomposition (with TGA), TPD, and CO_2 chemisorption at 250°C. CO_2 chemisorption at 250°C proved to be effective for the measurement of potassium dispersion but not for sodium. Using N_2O as the reactant facilitated the observation and analysis of the reaction mechanism of gas–carbon reactions due to its readiness for dissociative chemisorption and also because the C–N_2O reaction is an elementary reaction. Based on isothermal reactions and TPR, potassium was found to be more active in both N_2O dissociation and oxygen transfer thus gave rise to a much higher activity. It was found that K/C was an excellent catalyst for N_2O decomposition. In the low-temperature range of 150–250°C, a significant amount of N_2 was produced on K/C with no carbon gasification. Significant CO_2 production occurred only at higher temperatures. The fundamental reason for the difference in activities of the two alkali metals is a combination of three factors. First, K/C is highly active for N_2O dissociation. The O atoms thus produced would form active surface intermediates, most likely the epoxy intermediate which significantly weakened the surface C–C bonds for gasification (which is the basis of the unified mechanism of Chen and Yang). Second, the surface phenolate group also weakened the C–C bond to facilitate gasification, but the weakening was more pronounced by the –C–O–K group than by the –C–O–Na group. Third, the dispersion of K_2O on carbon was higher than that of Na_2O.

Key Words: **N_2O decomposition catalyst; alkali supported on carbon; carbon–NO_x reaction; catalyzed carbon–N_2O reaction.**

INTRODUCTION

It is well-known that alkali compounds are the best catalysts for the gasification of carbon or coal by CO_2 (to form CO) and H_2O (to form H_2 and CO) and extensive studies have been carried out in this area. In recent years, these compounds have also been investigated as catalysts for the reduction of nitric oxide and nitrous oxide with carbon. Kapteijn *et al.* (1) observed a large increase in NO reduction (and carbon reactivity) when Na, K, and Cs were added to the carbon, and the sequence of activity correlates with the order in the periodic table: Cs > K > Na. The same sequence was found in CO_2– or H_2O–carbon gasification catalyzed by alkali metals (2–4). Okukara and Tanaka (5) found that, upon potassium addition to activated carbon, both the NO adsorption capacity and carbon reactivity increased. Illán-Gómez *et al.* (6, 7) studied NO reduction by potassium-loaded activated carbon in detail and found that, similar to the carbon gasification by CO_2 or O_2, the catalytic role of potassium was also attributed to its effective participation in an oxidation–reduction (redox) cycle between K_xO_y and K_xO_{y+1}, in which the catalyst is oxidized by NO and reduced by carbon. Here, K_xO_y is a substoichiometric oxide in which the O/K ratio is lower than that of K_2O. A systematic study of a catalyzed C–NO reaction by alkali, alkaline-earth, and transition metals have recently been studied by Huang and Yang (8) using STM and molecular orbital theory. Catalysts for the C–NO reaction other than alkali metals, particularly Cu (9, 10), have also been investigated (11–14).

To the best of our knowledge, the only report on N_2O catalytic conversion to N_2 over alkali (or alkali-earth) catalysts supported on carbon at low temperature (<400°C) is the recent study by Zhu and Lu (15). In this study, potassium proves to be much more active and stable than either copper or cobalt because potassium possesses strong abilities both for N_2O chemisorption and oxygen transfer. A detailed analysis of the reaction mechanism and characterization of samples was conducted. Moreover, no report has appeared so far on a comparative study of various alkali catalysts supported on carbon, although such kinds of studies have been extensively conducted on CO_2– or H_2O–carbon gasification (3, 4, 16–19). As noted, Kapteijn *et al.* (1) compared the activities of Na, K, and Cs for NO–carbon reaction, but their study was too preliminary to give any mechanistic or characteristic analysis.

[1] To whom correspondence should be addressed. E-mail: maxlu@cheque.uq.edu.au. Fax: 61 7 33654199.

0021-9517/00 $35.00

Both N_2O– and NO–carbon reactions are actually gasification just like the CO_2– or H_2O–carbon reaction (19). Although the reactivity of these oxygen-containing reactants is different ($N_2O > NO > H_2O > CO_2$), they are very similar based on a redox reaction mechanism, and a unified theory of reactions of carbon with theses oxygen-containing molecules has been developed by Chen and Yang (19, 20). Because N_2O is a relatively simple oxidant, it is often used to evaluate the activities of various catalysts for oxidation reactions and as a probe for catalyst characterization (21–25). Consequently, the C–N_2O reaction is an elementary reaction while the C–NO reaction is not (16). In the study of the influence of acid treatments on N_2O conversion over copper catalysts supported on carbon (26), it was found that when the concentration of the acid solution was moderate (2 N), the influence of acid treatments on NO reduction could hardly be detected. However, N_2O reduction was quite sensitive to the same acid treatments. Therefore, the use of N_2O as an oxygen-containing reactant is very helpful, not only for the understanding of the fundamental mechanism but also from a practical standpoint. In this study, we conducted a comparative study of alkali catalysts for N_2O catalytic conversion with carbon. According to the literature (3, 4, 27–29), Na is similar to Li and K is close to Cs, while K is very different from Na in activity, dispersion, and other catalytic characteristics. So K and Na were selected in the present study due to their practical importance. By using N_2O as the oxygen-containing reactant, it is expected that we will be able to obtain an understanding of the differences among different alkali catalysts in activity, dispersion, and other characteristics.

EXPERIMENTAL

Catalyst preparation. The catalysts were prepared by impregnating activated carbon (Calgon BPL) with an aqueous solution of sodium nitrate and potassium nitrate (Ajax Chemicals, AR grade) at room temperature for 24 h. The sample was then dried at ca. 100°C overnight and finally decomposed at 300°C in He for 1 h. The sodium catalysts prepared with Na weight loadings of 5%, 12.5%, and 20% were referred to as Na5/AC, Na12.5/AC, and Na20/AC, respectively; similarly, potassium catalysts with K loadings of 5%, 10%, and 20% were designated as K5/AC, K10/AC, and K20/AC, respectively. Generally, catalysts with any sodium loading were referred to as Na/AC, with any potassium loading as K/AC, and the parent activated carbon without added sodium and potassium as AC.

Catalyst activity measurements. The N_2O carbon reaction was carried out under atmospheric pressure in a fixed-bed flow reactor (10-mm inside diameter; 200-mg sample), and the gaseous products were analyzed by a gas chromatograph (Shimadzu GC-17A) equipped with a heat conductivity detector and a Carbosphere column. Two modes of experiments were employed. The first was temperature-programmed reaction (TPR). The sample was first subjected to an *in situ* heat treatment in He at 25°C/min to 500°C and held at 500°C for 1 h; then the temperature was lowered to room temperature, followed by heating of the sample at 4°C/min to ca. 400°C in a N_2O/He mixture. The second was isothermal reaction at 320°C. The feed gas, with a gas hourly space velocity (GHSV) of 22,500 ml g^{-1} h^{-1}), contained 3000 ppm N_2O in He. The particle size was less than 0.08 mm in all reaction measurements to eliminate the internal diffusion resistance. Under GHSV = 22,500 ml g^{-1} h^{-1}, external diffusion also proved to be negligible, and quantitative calculation was conducted in the previous study (15).

Specific surface area and pore volume measurements. The N_2 adsorption/desorption isotherms at −196°C were obtained using a gas sorption analyzer (NOVA 1200, Quantachrome). Samples were degassed for 3 h at 300°C prior to the adsorption analysis. The BET surface area (S_{BET}) and total pore volume (V_{total}) were obtained from the adsorption isotherms. The t-plot method was used to calculate the micropore volume obtained from N_2 adsorption ($V_{m\text{-}N2}$). CO_2 adsorption at 0°C was made with the same analyzer. The DR method was used to calculate the volume of micropores obtained from CO_2 adsorption at 0°C ($V_{m\text{-}CO2}$).

CO_2 chemisorption and thermal decomposition of catalysts. Thermogravimetric analysis (TGA) experiments were carried out in a thermobalance (Shimadzu TGA-50). Samples were loaded into a platinum pan and heated under helium from room temperature to 110°C, held at that temperature for 20 min, and then heated to 900°C with a heating rate of 10°C/min to obtain a decomposition profile of the K catalyst; or to 500°C and held for 1 h, followed by CO_2 chemisorption at 250°C. The procedure of CO_2 chemisorption was described in detail by Illán-Gómez *et al.* (6).

Temperature-programmed desorption (TPD). TPD experiments of selected supports and catalysts were carried out in a vertical tube furnace with He as the carrier gas. A 1-g sample was placed in a quartz tube, heated to 110°C for 60 min, and then heated at 5°C/min to 900°C. The gases evolved were continuously analyzed using a chromatograph (Shimadzu GC-17A) equipped with a thermal conductivity detector and a Carbosphere column.

RESULTS

Isothermal Reactions

The results of the isothermal reactions over pure AC, Na/AC, and K/AC at 320°C are compared in Fig. 1. In all cases, the carbon burnoff was less than 4% over the time period of 150 min. It is seen that the activity of pure AC at 320°C was negligible (2% N_2O conversion). Impregnation of Na or K improved the activity, and the following

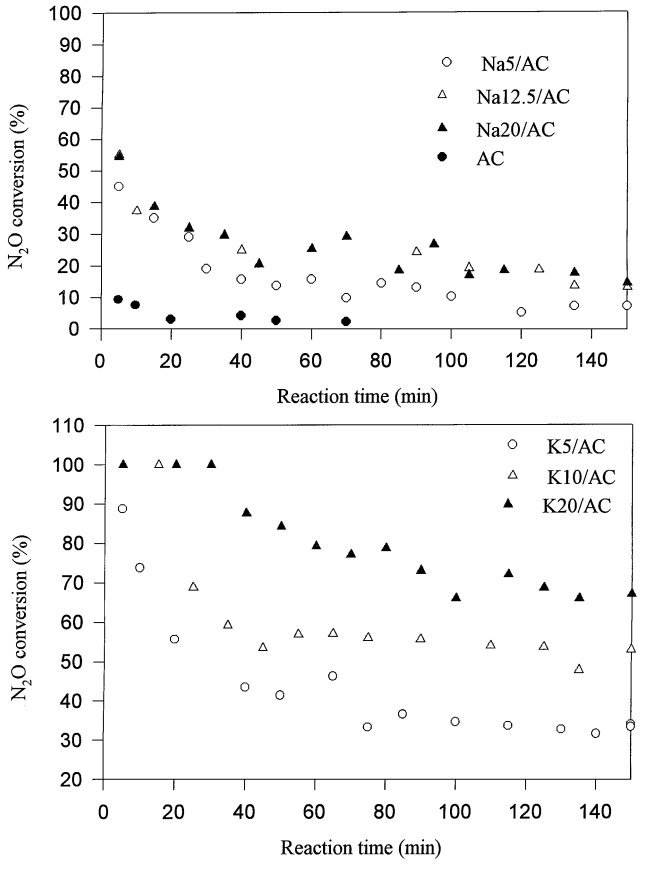

FIG. 1. Isothermal reactions on activated carbon (AC), Na on carbon (Na/AC, number indicates wt%), and K on carbon (K/AC). Reaction conditions, 320°C; space velocity, 22,500 ml/g/h; feed, 3000 ppm N_2O/He. Carbon burnoff <4% in all cases.

common features were shared by both Na/AC and K/AC catalysts. First, the activities were very high initially, followed by a gradual decrease until a constant level of N_2O conversion was reached. Secondly, the catalyst loading affected the activities. Generally, a higher loading not only prolonged the initial high activity period but also leveled off to a higher N_2O conversion. However, the following differences were also seen. For Na/AC, 12.5 wt% Na did not improve the activity very significantly over that with 5 wt% Na and a higher loading beyond 12.5 wt% Na did not further increase the activity. For K/AC, a progressive improvement in activity with increasing loading was observed. Another difference is that potassium was much more active compared to sodium at the same catalyst loading. For example, with 20 wt% loading, potassium yielded around 70% N_2O conversion, compared with 20% N_2O conversion for Na20/AC under the same conditions. As noted in the introduction, the recent study by Zhu and Lu (15) also presented a comparison of activities among potassium, copper, and cobalt. It was found that potassium was even more active than Cu and Co. With 20 wt% loading, potassium yielded approximately 97% N_2O conversion at 350°C while Cu and Co showed about 75% conversion under the same conditions; pure AC gave only 5% N_2O conversion. Meanwhile, potassium also showed better stability in activity compared with either Cu or Co. The higher activity and stability of potassium were attributed to the stronger ability of potassium in N_2O chemisorption and oxygen transfer from catalyst to carbon in the redox cycle. To compare the activity of Na with that of copper and cobalt, the reaction temperature was deliberately increased to 350°C for Na20/AC and only 35% N_2O conversion was obtained. Hence, it was concluded that sodium was less active than copper and cobalt.

TPR Experiments

TPR profiles of the N_2O–carbon reaction on pure AC and M/ACs (M = metal) are compared in Fig. 2. No N_2O conversion was observed over pure AC until ca. 440°C and the temperature required for reaching 100% N_2O conversion (T_{100}) was over 600°C. Impregnation of M caused a substantial decrease both in the starting reaction temperature and the T_{100}. For Na/AC, the reaction started vigorously above 300°C and T_{100} was lowered to ca. 420°C. For K/AC, significant reaction began around 250°C and 100% N_2O conversion was reached at near 370°C. An increase in K loading

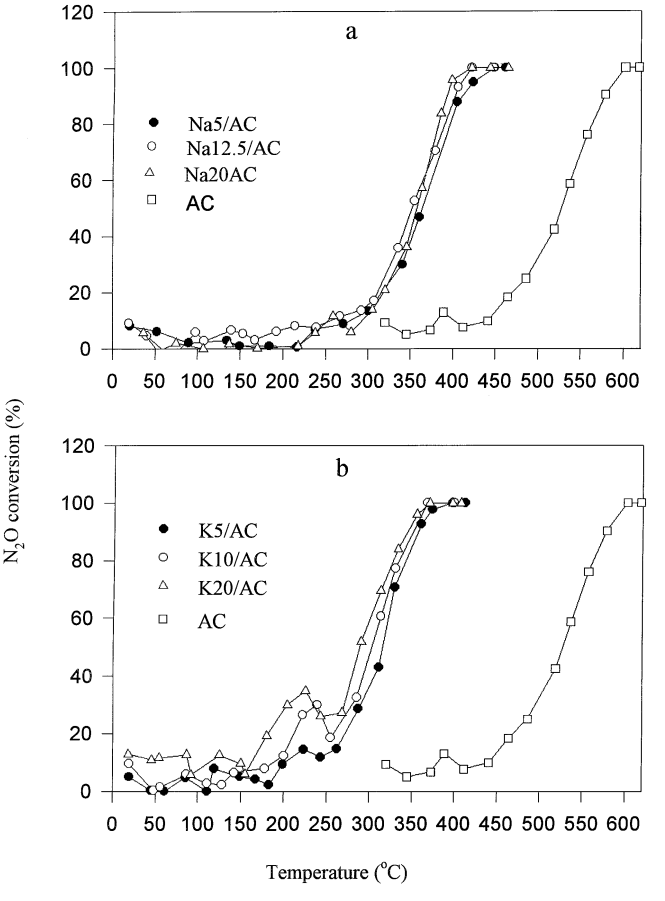

FIG. 2. TPR profiles of Na/AC (a) and K/AC (b). Feed: 3000 ppm N_2O/He. Heating rate = 4°C/min. See Fig. 1 for other conditions.

from 5 to 20 wt% progressively shifted the TPR plots to lower temperatures. In contrast, the TPR plots of Na/AC were slightly shifted toward lower temperatures when the loading was increased from 5 to 12.5 wt%, and the TPR plots of Na20/AC and Na12.5/AC were nearly the same. This trend coincided with that obtained for the isothermal reactions. As Na12.5/AC and K20/AC had the same C/*M* atomic ratio (0.075) and Na12.5/AC showed the maximum activity for the Na/AC catalysts, we will focus mainly on K20/AC and Na12.5/AC (unless otherwise stated) in the following comparison of sodium and potassium catalysts.

Product Analysis

Analysis of TPR products provides important information on the reaction. Figure 3 shows the evolution of products during a TPR experiment over Na12.5/AC and K20/AC. We found that the CO_2 selectivity defined as $100\% \times CO_2/(CO_2 + CO)$ was 100% during the whole TPR experiments; i.e., no CO was detected in the products. Because one N_2O molecule reacting with carbon produced one N_2 but only 0.5 CO_2, the number of moles of N_2 was twice that of CO_2 if no oxygen was retained on the surface. To better show the oxygen balance in the product analysis, the CO_2 concentration was multiplied by 2. In this manner, the CO_2 concentration was equal to that of N_2 in the products if there was no delay for oxygen-containing products. In Fig. 3b, four regions of reactivity over K20/AC are observed:

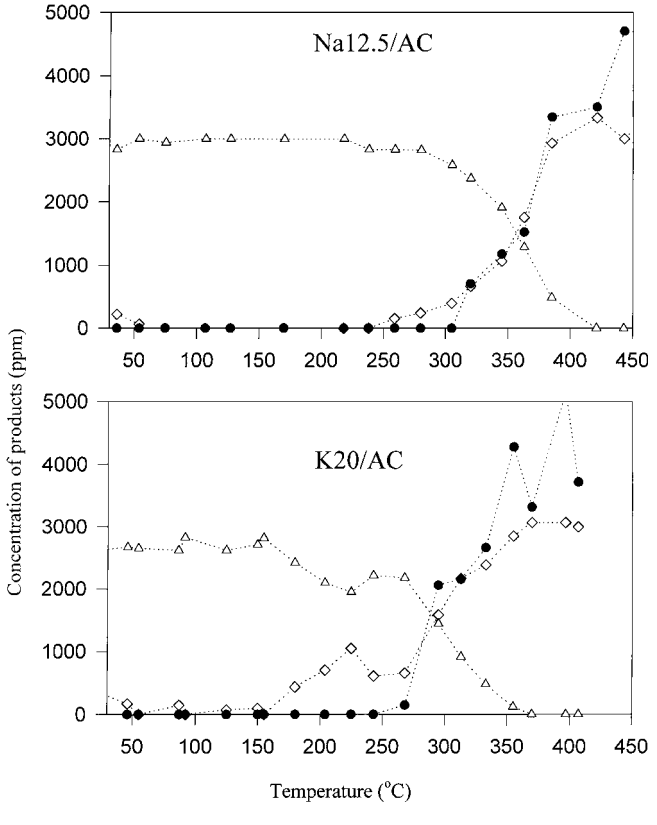

FIG. 3. Product analysis during TPR (see conditions in Figs. 1 and 2) (●, $2CO_2$; △, N_2O; ◇, N_2).

(I) The first stage was characterized by a low conversion of N_2O and a very small evolution of N_2 ($T <$ ca. 50°C). However, no oxygen-containing products other than N_2O were found, and the oxygen from N_2O decomposition was retained on the K/AC catalyst. Obviously, this was due to an irreversible dissociative chemisorption of N_2O on potassium oxide particles, which was also observed on Ni (30) and Cu (31) at similarly low temperatures. Non dissociative chemisorption or physical adsorption could also be observed in this region based on the negative N_2 balance.

(II) In the second stage ($50 < T < 150$°C), chemisorption seemed to be saturated, for N_2 almost disappeared and N_2O conversion was negligible; no more oxygen accumulation occurred in this stage.

(III) In the third stage ($150 < T < 250$°C), the N_2 peak re-appeared, but it was much stronger compared with that in the first stage. The oxygen balance was still negative in this stage, for no CO_2 was observed.

(IV) The fourth stage was characterized by the appearance of CO_2 at ca. 250°C, from which temperature N_2 started to increase almost linearly until 100% N_2O conversion was reached at ca. 370°C. However, CO_2 increased more rapidly than N_2 as an excess of CO_2 evolution with respect to N_2 was observed at ca. 270°C. So the oxygen balance was still negative below 270°C, but became positive afterward.

Similar reaction stages were observed for Na12.5/AC except for the following differences. (1) The N_2 peak in the first stage was relatively smaller than that of K20/AC. (2) In the third stage, the temperature for the re-appearance of the N_2 peak was 230°C over that of Na12.5/AC, which was much higher than 150°C for K20/AC. (3) The starting temperature for CO_2 appearance over Na12.5/AC was 300°C, which was 50°C higher than that over K20/AC. (4) The excess in CO_2 evolution with respect to N_2 did not appear until nearly 370°C for Na12.5/AC, which was also much higher than 270°C for K20/AC.

Oxygen balance can provide very useful information for understanding the reaction mechanism. As discussed in a recent study (15), during the 500°C heat treatment in helium for 1 h, the catalyst precursor was reduced by carbon to a substoichiometric oxide K_xO_y. In Fig. 3, during TPR, the oxygen balances were negative during the first stage, the third stage, and the initial part of the fourth stage (below ca. 270°C for K20/AC). This negative oxygen balance indicates oxygen accumulation and formation of more oxidized K_xO_{y+1}. Our previous study showed that the negative oxygen balance in the first stage was due to oxidation of the surface of the catalyst particles while the oxidation of the bulk catalyst particles resulted in negative oxygen balance

in the third and fourth stages. In the fourth stage, above ca. 270°C over K20/AC, oxygen balance became positive, indicating a release of oxygen that was accumulated in the previous stages. As the surface complexes remaining on the carbon surface following the initial 500°C heat treatment were unstabilized in the presence of a N_2O atmosphere, a much higher excess of CO_2 release with respect to N_2 was observed after 100% N_2O conversion was reached. This phenomenon was also observed by Illán-Gómez *et al.* (6).

The redox cycle mechanism described above is also applicable to Na12.5/AC based on the occurrence of the similar reaction stages. The four aspects (noted above), in which the evolution of products during TPR over K20/AC and Na12.5/AC differed, provide quite useful information on the reason why the K catalyst is more active than the Na catalyst. The larger N_2 peak in the first stage over K20/AC means that the K catalyst possesses a stronger ability for N_2O dissociative chemisorption. This was confirmed by the earlier and also much larger N_2 peak in the third stage over K20/AC compared to that over Na12.5/AC. Moreover, CO_2 evolution started at a much lower temperature over K20/AC compared to that over Na12.5/AC, indicating that oxygen transfer from the catalyst to the carbon and the release of surface carbon–oxygen complexes could proceed much more easily over K/AC than over Na/AC. This was further evidenced by the earlier excessive CO_2 evolution with respect to N_2 for K20/AC. A more detailed discussion on the difference between the activities of Na/AC and K/AC will be presented later.

In Fig. 4, a delay in the evolution of CO_2 with respect to N_2, was observed during the isothermal reaction at 320°C with both Na12.5/AC and K20/AC (both were subjected to 500°C heat treatment in He before the reaction). After the initial stage, CO_2 production rose to the stoichiometric ratio with N_2. This confirms the above redox cycle mechanism. Before the reaction, a reduced form of M_xO_y was produced by the 500°C heat treatment (in He) on the reducing carbon surface. This reduced M_xO_y could accept oxygen from N_2O and be oxidized into M_xO_{y+1} at the reaction temperature of 350°C. One hundred percent N_2O conversion could continue until no more oxygen could accumulate on the potassium oxides and such a steady-state redox cycle of M_xO_y/M_xO_{y+1} was reached. We also note that the delay over K20/AC was much larger than that over Na12.5/AC, and it also lasted a longer time. This suggests that potassium possessed a much stronger ability in dissociating N_2O than sodium.

Pore Structure

Table 1 shows the surface area and pore structure of samples heat-treated at 500°C in helium for 60 min. Most pores were micropores for AC and *M*/AC, and the increasing loading of *M* caused a progressive decrease not only in total surface area and total pore volume but also in micropore

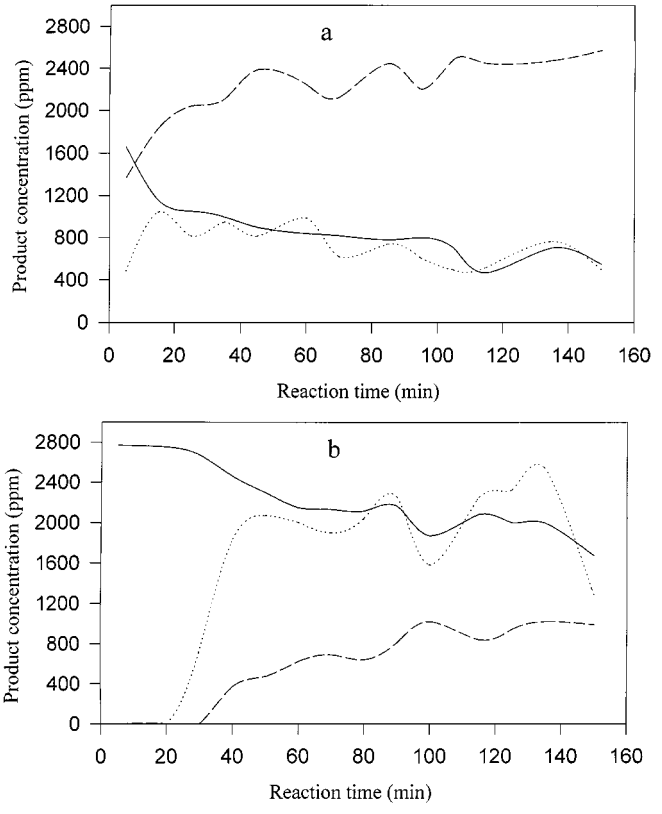

FIG. 4. Product analysis during isothermal reaction at 320°C for (a) Na12.5/AC and (b) K20/AC. The two samples had the same M/C ratio (see Fig. 1 for other conditions) (. . . , $2CO_2$; - - -, N_2O; —, N_2).

volume (obtained from N_2 adsorption at −196°C and CO_2 adsorption at 0°C). Because the decreases were obviously not due to collapse of the pore structure of activated carbon by heat treatment at 500°C in He, they must have resulted from the blockage of pores by the small *M* particles.

The percentages of decrease in pore volume due to impregnation of catalysts are shown in Fig. 5. Observation reveals common characteristics between Na/AC and K/AC in that the percentages of decrease in the total pore volume and micropore volume were not the same after the impregnation of either Na or K. This means that the dispersion of catalysts in carbon was not very uniform. However, for

TABLE 1

Specific Surface and Pore Volume (V_{total}, Total Pore Volume; V_m, Micropore Volume)

Samples	S_{BET} (m^2/g)	V_{total} (cc/g)	$V_{m\text{-}N2}$ (cc/g)	$V_{m\text{-}CO2}$ (cc/g)
AC	1077	0.510	0.408	0.236
Na5/AC	952	0.446	0.365	0.238
Na12.5/AC	914	0.428	0.349	0.217
Na20/AC	696	0.331	0.268	0.146
K5/AC	898	0.436	0.340	0.195
K10/AC	803	0.397	0.301	0.158
K20/AC	646	0.341	0.247	0.130

Na/ACs, the percentage of decrease in V_{total} was slightly larger than that in $V_{m\text{-}N2}$ at all catalyst loadings, while K/ACs showed lower percentage reductions in V_{total} than in $V_{m\text{-}N2}$. This indicates that Na particles were more likely to stay in the outside spaces of the pores, while K could migrate into the inner micropores more readily and consequently yield a more uniform dispersion. N_2 and CO_2 do not measure the same type of microporosity (32, 33). CO_2 data give the micropores ($V_{m\text{-}CO2}$) and N_2 data provide the total micropore volume ($V_{m\text{-}N2}$) including the supermicropores. It is seen that the percentage decrease in $V_{m\text{-}CO2}$ was even more than that in $V_{m\text{-}N2}$ for K/AC, whereas Na/ACs showed a much lower reduction in $V_{m\text{-}CO2}$ than in $V_{m\text{-}N2}$ except for Na20/AC. The exception for Na20/AC was related to the sintering of metal (as will be discussed later), so the micropores with pore volume $V_{m\text{-}CO2}$ were partially blocked. This comparison further suggests that the potassium catalyst particles could more readily migrate into $V_{m\text{-}CO2}$ while the sodium catalyst mostly distributed in the supermicropores or mesopores.

Thermal Decomposition

The thermal decomposition curves in weight losses of Na12.5/AC and K20/AC (obtained by TGA) are shown in Fig. 6. For both samples, there was a sharp peak at ca. 400°C, and a broad one starting from ca. 600°C. The former corresponded to the decomposition of nitrates into oxides (and subsequent reactions of carbon with nitrogen oxides from the nitrates). The latter peak indicates the reduction of oxides by carbon, and the reduction of both sodium oxides and potassium oxides was negligible below 600°C. The TPD results (Fig. 7) show that the peaks of weight loss above 600°C were mainly due to the evolution of CO rather than CO_2. We also note that there are two shoulders in the second broad peak for Na12.5/AC (at 700 and 800°C, Fig. 6), suggesting the existence of different Na species. The shoulder at the lower temperature is attributed to relatively small particle sizes, which had better contacts with carbon, while larger particles were responsible for the shoulder at the higher temperature. This is confirmed by TPD results (Fig. 7) in which two shoulders that resulted from CO evolution over Na12.5/AC were clearly observed at nearly the same positions as those in the TGA experiment. Figure 7 also shows two shoulders in the second broad peak of K20/AC, but they are not as apparent as those in the case for Na12.5/AC. A similar phenomenon over potassium catalysts supported on activated carbon was observed by Illán-Gómez *et al.* (6). The previous observations indicate that although the reduction of both sodium oxide and potassium oxide started at nearly the same temperature, the latter proceeded more readily because of better dispersion of the potassium catalyst compared to that of sodium catalyst.

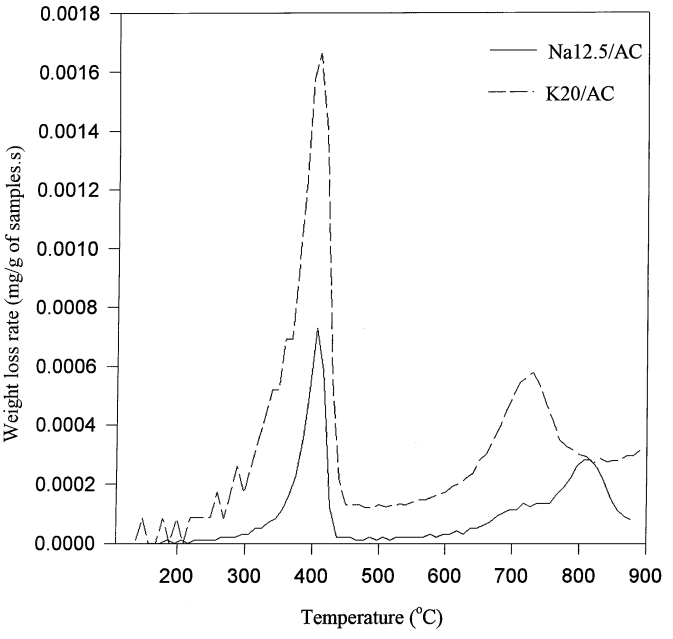

FIG. 6. Weight loss rate of Na12.5/AC and K20/AC in He at a heating rate of 5°C/min.

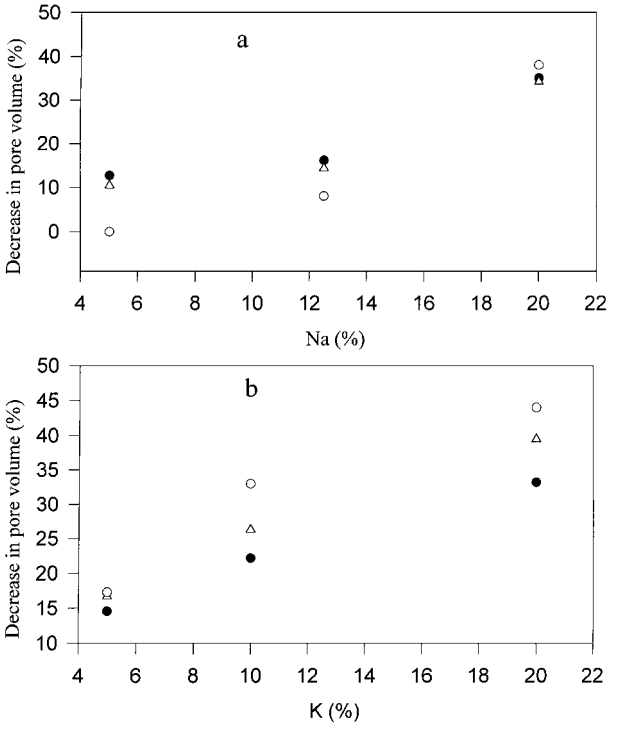

FIG. 5. Decrease in pore volumes due to impregnation of Na (a) and K (b), expressed in wt% metal oxide. V_{total}, total pore volume; V_m, micropore volume by N_2 and CO_2 (●, V_{total}; △, $V_{m\text{-}N2}$; ○, $V_{m\text{-}CO2}$).

DISCUSSION

CO_2 Chemisorption and Specific Rates

CO_2 chemisorption (at 300°C) has been attempted for measurement of the active site densities of alkali catalysts

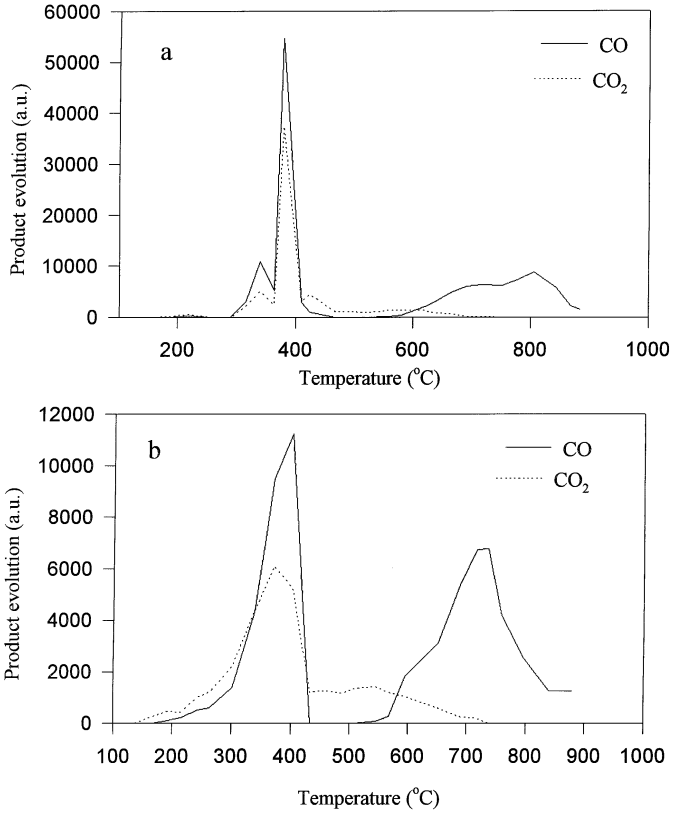

FIG. 7. TPD of (a) Na12.5/AC and (b) K20/AC in He at a heating rate of 5°C/min.

on coal at intermittent periods of coal gasification and based on which a constant turnover number was obtained (34). The same method was successfully used to characterize the external surface and the dispersion of calcium particles on carbon (35). On the contrary, Illán-Gómez *et al.* encountered problems when they tried to use CO_2 chemisorption as a means to study the dispersion and active sites density of potassium supported on activated carbon for NO reduction (6, 7). In one case (Table 3, Ref. 6). They found that CO_2/K_2O decreased with decreasing K loading when they used different carbon supports. In another case (Table 1, Ref. 7) they found that CO_2/K_2O was constant with increasing amounts of potassium supported on the same carbon. In the recent study of Zhu and Lu (15) on N_2O decomposition over K/AC, CO_2 chemisorption proved to be very effective for the characterization of dispersion of the K catalyst because the data of turnover frequency based on CO_2 chemisorption at 250°C fell on a single line very well. By a detailed analysis, the problem of Illán-Gómez *et al.* could be understood. First, a comparison of dispersions of potassium on different carbon materials would not be meaningful because the dispersion is affected by various factors such as pore structure, surface chemistry, and mineral contents. Second, the catalyst loadings that were used were too low (<7.4 wt%), so they failed to observe any trend of catalyst dispersion since potassium can disperse so well on carbon that the dispersion of catalyst would be independent of catalyst loading on the high-surface-area substrates (36) and at relatively low catalyst loadings (37).

Chemisorption of CO_2 at 250°C was conducted after a heat treatment at 500°C in helium for 1 h and the results are shown in Table 2. It is seen that with increasing K loadings from 5 to 20 wt%, CO_2 adsorbed per gram of sample increased. However, for Na, only a small increase in CO_2 adsorption was observed when the loading increased from 5 to 12.5 wt%, and a decrease was observed upon further increasing of the loading to 20 wt%. Such a trend was also observed by Cerfontain *et al.* (28). The decreasing amount of CO_2 chemisorption with loading indicates the sintering of the sodium particles at high loadings. More direct evidence for the sintering of Na was observed during the preparation of catalyst samples when white spots in Na20/AC were seen after the heat treatment. These white spots were apparently clusters of sodium particles caused by sintering. For convenience in analysis, we assume that one CO_2 was adsorbed on one M_2O site to form a surface carbonate, although from a previous discussion (15), it was substoichiometric M_xO_y instead of M_2O that actually existed. A decreasing ratio of CO_2/M_2O with increasing M loading was observed for K/AC (column 3 in Table 2), which indicates decreasing dispersion with loading. However, we cannot compare the dispersions of Na and K simply based on the amount of CO_2 chemisorption because the numbers of Na and K for chemisorbing one CO_2 molecule may be different. Previous studies (28, 29, 34, 38) have shown that one CO_2 molecule was chemisorbed on three or four K atoms. But to the best of our knowledge, there have been no reports on the number of Na atoms for chemisorbing one CO_2 molecule.

As N_2O conversion varied during the isothermal reactions (see Fig. 1), the specific activities are based on the average activities during the entire 150-min isothermal reaction. A comparison of the specific activities is presented in Fig. 8. Figure 8a reveals two facts: (1) K/ACs gave a much higher specific activity per gram of sample than Na/ACs at the same weight loadings. (2) From 5 to 20 wt% loadings, K/ACs showed a continuing increase in activity, while for Na/ACs a loading of more than 12.5% could not further

TABLE 2

CO_2 Adsorption at 250°C

Samples	CO_2 adsorbed (μmol/g of sample)	CO_2/M_2O
Na5/AC	203	0.187
Na12.5/AC	235	0.108
Na20/AC	190	0.043
K5/AC	159	0.248
K10/AC	216	0.169
K20/AC	311	0.129

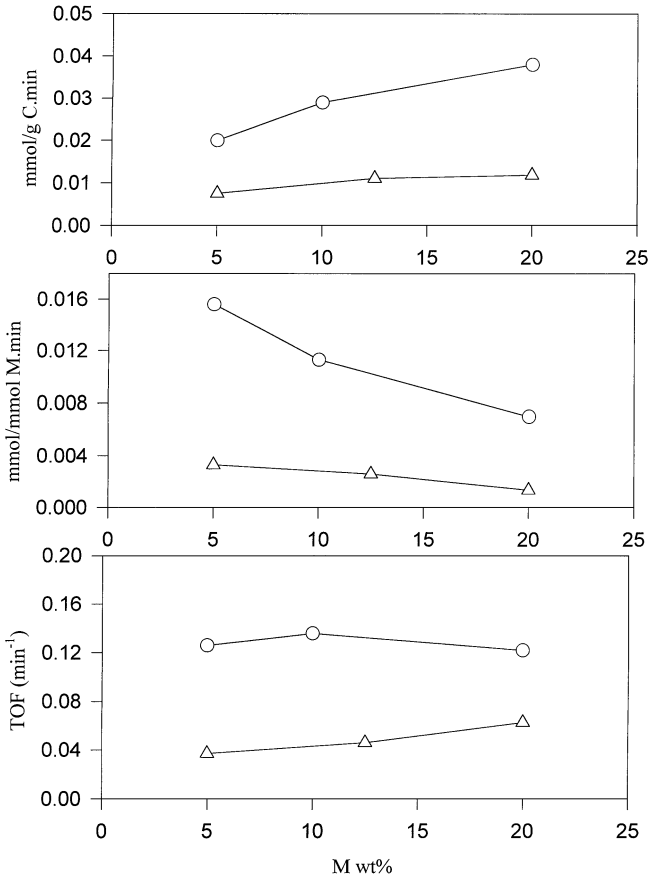

FIG. 8. Specific rates of N_2O reduction (in mmol of N_2O reduced) on Na/AC and K/AC at 320°C, where *M*:C represents the atom ratio of Na or K to carbon (△, Na/AC; ○, K/AC).

increase the specific activity. Figure 8b shows that potassium also possesses a higher specific activity than sodium on a per *mmol* metal basis. Another important observation from Fig. 8b is that the specific activity per mmol of metal decreased with increasing loading for both K/ACs and Na/ACs. This suggests decreasing dispersion with increasing catalyst loading, which is in agreement with the results from CO_2 chemisorption. Figure 8c shows the turnover frequencies (TOF) based on surface metal sites determined by CO_2 chemisorption at 250°C. It is seen that the potassium catalysts also possessed much higher turnover frequencies compared to sodium catalysts. More importantly, we note that the turnover frequencies were nearly constant over K/ACs with different potassium loadings. However, for sodium catalysts, the turnover frequencies increased with increasing loading. Therefore, it is concluded that CO_2 chemisorption at 250°C is a very effective means for measuring the dispersion of K catalysts supported on carbon. This was also reported in a previous study by Zhu and Lu (15). However, for sodium catalysts, this method failed. The reason is two-fold. First, compared with potassium, sodium could more easily form carbonate crystals (27). Another reason may be related to the sintering of sodium as observed.

Activation Energy, Catalyst Dispersion, and Unified Mechanism

The mechanism of alkali-metal-catalyzed gasification of carbon by oxygen-containing reactants has been the subject of much discussion. One argument is that the catalyst increases the number of active sites at the carbon surface without fundamentally changing the kinetic network. The evidence is that the "Arrhenius plots" run essentially parallel in the CO_2–carbon gasification either uncatalyzed or catalyzed by alkali metals (3, 4), indicating the same activation energy. Hence, the differences in activities was explained by a different number of active sites produced by different alkali catalysts, contained in the pre-exponential factor k_0. The catalytic activity correlates with the order in the periodic table: Cs > K > Na > Li.

Molecular orbital theory calculations for graphite oxidation have significantly advanced the understanding of the reactivity and structure of the carbon active sites and surface O complexes (19, 39–41). The calculations show that due to these chemisorbed oxygen atoms, the neighboring (and surface) C–C bonds are weakened significantly; hence, carbon is freed from the structure. Similar calculations were performed to understand the mechanism of catalysis by alkali metals (8, 19, 42). The active carbon sites are the edge atoms on the armchair and the zigzag faces. For both faces the structure with potassium or other metal phenolate (–C–O–K or –C–O–*M*) groups are considered. From the calculations it appeared that with or without potassium (or *M*), the C–C bonds on the surface were both significantly weakened. The differences among the different metals are not very significant. Therefore one would not expect a clear decrease in the activation energy by potassium. More importantly, a off-plane O species bonded to the saturated edge carbon atom was highly stable and hence was proposed by Yang *et al.* (19, 39–41) as the key intermediate. This intermediate could substantially weaken the surface C–C bonds, and the C–C bond breakage was the rate-limiting step for gasification. More recently, an epoxy oxygen intermediate was found to be even more stable by Chen and Yang (20). Hence, this epoxy intermediate was proposed as the key intermediate. Based on this epoxy intermediate, a unified mechanism for all gas-carbon reactions with oxygen-containing reactants has been proposed by Yang *et al.* Such a mechanism could explain all uncatalyzed as well as catalyzed reactions. The epoxy oxygen intermediate could be formed by O atoms that are supplied by dissociation of the oxygen-containing reactant (either uncatalyzed, i.e., on the step carbon atoms, or on catalysts). The concentration of the epoxy species on the carbon surface would determine the activity of gaseous reactant (20). For catalyzed reactions with H_2O and CO_2, molecular orbital calculations

(19) showed the weakening of the C–C bonds followed the correct rank order: K > Na > Li. For catalyzed C–NO reactions, molecular orbital theory predictions showed the following rank order: K > Ca > Cu > Na > Li, which agreed with experimental results (8).

AES studies have shown evidence of intercalation of K in graphite at temperatures as low as 310 K (43, 44). It was suggested (29) that stabilization of the alkali metal during heat treatment could be obtained through intercalation. The differences in alkali metal interaction observed in this study corresponded to the fact that Na forms only a lower stage intercalation compound ($C_{64}Na$) compared to Cs and K (C_8K, C_8Cs). Hence, the amount of Na that can enter the carbon matrix is much lower than the amount of K and Cs; thus, Na mainly interacts with the easily accessible oxygen present on the reactive surface. The interaction of alkali with the oxygen complex on carbon is a second factor that determines the amount of alkali metal that can be stabilized. Lang (27) showed that alkali phenolate formation is most favorable for Cs, followed by K and Na. This could be a reason as to why Cs or K can supply more active sites (or shows a much better dispersion) than Na.

Despite the above qualitative analysis, to the best of our knowledge, quantitative results are not available on the comparison of the different dispersions or active sites of different alkali metals. In the measurement of catalyst dispersion using a surface alkylation technique, Mims and Pabst (38) obtained only qualitative conclusions, that the difference between the absolute rates of the sodium- and potassium-catalyzed samples was due in large part to differences in dispersion. In the present study, although the better dispersion of potassium compared to that of sodium could be qualitatively seen from the results on pore structures and thermal decomposition results, a quantitative comparison is still not available.

N_2O Dissociation

In the present study, N_2O instead of CO_2 or H_2O was used as the gas reactant. N_2O can be dissociatively chemisorbed more readily than CO_2 and H_2O. The produced N_2 could also be more easily distinguished from other gases; hence, we could observe separate processes of N_2O chemisorption and oxygen transfer. Dissociative chemisorption of CO_2 or H_2O requires high temperatures, and the products are also not easy to analyze because CO or CO_2 can evolve either in the presence or in the absence of CO_2 (or H_2O) during the reaction. Therefore, N_2O is a more effective test agent for studying the reaction mechanism. Indeed, in the present TPR experiments, the separate processes of N_2O dissociative chemisorption (judging by N_2) and O transfer (judging by CO_2 appearance) were clearly delineated. If CO_2 or H_2O were used, such separate processes would be impossible to observe. In Fig. 3, N_2O dissociative chemisorption more readily occurred on K20/AC than on Na12.5/AC (these two catalysts had the same C/*M* atomic ratio). This can be explained by recalling the mechanism of N_2O dissociation on active sites. Dissociative chemisorption of N_2O on the catalysts' active centers is generally envisaged as electron donation from the catalyst into the antibonding orbitals of N_2O, destabilizing the N–O bonding and leading to scission. Metal surfaces, oxides with local charge donation properties, and isolated transition metal ions with more than one valence can act as such centers. Actually, O_2 (and NO) dissociation on catalysts is also based on the same mechanism (45, 46). As K has a lower electronegativity than Na, dissociative chemisorption of gas molecules (including N_2O, O_2, NO) would occur more readily on K (46). This could explain that the N_2 evolution peak re-appeared at a much lower temperature over K20/AC (150°C) than over Na12.5/AC (230°C) in the third stage of TPR (Fig. 3). The difference in dispersion of K and Na cannot account for this result. If the difference between K and Na catalysts only resulted from different dispersions, then the N_2 peak should have started at nearly the same temperature over K20/AC and Na12.5/AC in the third stage of TPR. However, the larger size of the N_2 peak in both the first and the third stages of TPR for K20/AC than that for Na12.5/AC was most likely caused by better dispersion of the potassium catalyst.

The above analysis of electronegativity suggests that Na sites do not possess the same activity as K sites. This can also be confirmed from the thermodynamic analysis. Assuming that the active sites are M_2O, N_2O chemisorption can be described as follows:

$$Na_2O + N_2O \rightarrow Na_2O_2 + N_2; \quad [1]$$

$$K_2O + N_2O \rightarrow K_2O_2 + N_2. \quad [2]$$

The Gibbs free energies are

$$\Delta G^\circ[1] = -175.9 \text{ kJ/mol}, \quad \Delta G^\circ[2] = -207.6 \text{ kJ/mol}.$$

It is seen that Reaction [2] has a more negative Gibbs free energy than Reaction [1], which means Reaction [2] is more favorable thermodynamically, i.e., a larger equilibrium constant. Therefore, the K sites should have a higher activity than Na sites for N_2O chemisorption.

Moreover, the relatively better dispersion of K, which was reflected in the analysis of pore structure and thermal decomposition of catalysts in the present study and also reported previously (3, 4, 27, 29), is also related to the lower electronegativity. K has a stronger electrostatic attraction to the surface oxygen on carbon than Na during impregnation (46). The stronger bonding of K to the surface oxygen decreases its possibility for agglomeration during reduction (activation), thus resulting in better dispersion. This is in good agreement with the explanation of Meijer *et al.* (29) as noted previously. Indeed, the dispersion of catalysts (and consequently the number of active sites) is critically

important to the whole redox cycle of the reaction. A better dispersion is beneficial not only to N_2O chemisorption by supplying a larger number of chemisorption sites but also to oxygen transfer from the catalyst particles to the carbon surface by providing more catalyst–carbon interfaces. The oxygen transfer to the carbon surface forms O intermediates which weaken the neighboring C–C bonds, thus prompting the release of surface complexes (in the form of CO_2). It is also worth noting that oxygen transfer affects N_2O chemisorption. If oxygen accumulated on the surface of catalyst particles is not removed in a timely fashion, N_2O chemisorption would be inhibited. A quick oxygen release from the catalyst particles facilitates N_2O chemisorption.

From the previous discusison, we find the previous conclusion (3, 4) that the differences in activities of different alkali metals were due to different densities of active sites simply based on their close or similar activation energies to be misleading.

Although the recent work of Chen and Yang (19) and Huang and Yang (8) is related more to the intrinsic properties of alkali metals, they did not consider the different abilities of alkalis in dissociative chemisorption of oxygen-containing gas molecules. In the presence of alkalis, the dissociative chemisorption of oxygen-containing molecules is mainly through the alkali particles instead of directly through carbon sites. This is clearly shown in the present study by product analysis during TPR of N_2O with alkali-loaded carbon (see Fig. 3). However, as CO_2 and H_2O were used in the work of Chen and Yang (19) and NO was used by Huang and Yang (8), such an observation was simply not possible. Another important issue (which was not addressed in their work) is the dispersion of catalysts, which has proven to be important for not only chemisorption of gas molecules but also oxygen transfer from catalyst particles to carbon sites. In this work, we suggest that the differences in activities of the various alkali metals are due to a combination of intrinsic properties and different numbers of active sites. During the redox cycle, the electronegativity of a metal plays a role. First, because of the low electronegativity, K sites are more active than Na sites in the first reaction step—N_2O chemisorption. Second, the lower electronegativity of K also contributes to better dispersion of K (or a larger number of active sites), which promotes not only oxygen transfer from catalyst to carbon and release of carbon–oxygen complexes from carbon surface but also N_2O dissociative chemisorption, thus improving the redox cycle efficiency.

Mechanistic Insights

Alkali and alkaline-earth metal oxides are not active for N_2O decomposition in comparison to oxides of transition and rare-earth metals (47–49). Carbon alone is also not active in N_2O decomposition, as significant decomposition on pure carbon can occur only above 400°C (50). When K_2O was supported on carbon, however, K/C showed high N_2O decomposition activities. The results given in Fig. 3 show that, in the low-temperature range of 150–250°C, approximately 30% of the N_2O was decomposed into N_2 on K_2O/C (at the high space velocity that was used), with no occurrence of carbon gasification (since no CO_2 was produced). Such a high activity for N_2O decomposition was clearly unmatched by the most active transition metal oxides.

In the study of Chen and Yang (42) on an alkali-catalyzed C–H_2O reaction, it was clearly shown that the surface phenolate group (–C–O–K) is not as active as clusters of K_2O (or K_xO_y), indicating that K_2O clusters are more active in H_2O dissociation to form O atoms. The results shown in Fig. 3 indicate that K_2O clusters supported on carbon are also excellent catalysts for N_2O dissociation (into N_2 and O). The carbon substrate is obviously necessary, and its contribution to the N_2O (or H_2O) dissociation actvity is two-fold: (1) carbon serves as a scavenger or trap for O atoms and (2) carbon reduces the oxidation state of K in the clusters (forming substoichiometric K oxides).

The O atoms are bonded to the carbon substrate to form surface oxygen complexes or intermediates, such as semiquinone and carbonyl groups. As mentioned previously, a stable epoxy oxygen intermediate has been proposed by Chen and Yang (20). The epoxy oxygen intermediate can significantly weaken the surface C–C bonds (by $\frac{1}{3}$ to $\frac{1}{2}$, for zigzag and armchair edges, respectively), thereby facilitating gasification of carbon. This was the basis for the unified mechanism of carbon gasification by all oxygen-containing molecules proposed by Chen and Yang (19, 20, 39, 41). The mechanism of the catalyzed C–N_2O reaction can also be described in terms of this unified mechanism. The dissociation of N_2O generates O atoms which form the epoxy oxygen intermediates. The carbon gasification rate as well as the activation energy of the reaction are related to the abundance of the epoxy oxygen intermediate (20). The activation energy of the C–O_2 reaction is of the order of 40–50 kcal/mol, which is the C–C bond energy with an epoxy oxygen intermediate. The activation energy of the C–H_2O and C–CO_2 reactions is near 80 kcal/mol, which is the C–C bond energy without the epoxy oxygen intermediate. The C–C bond energies mentioned previously are those of the zigzag edges of graphite. The corresponding values for the armchair edges are substantially lower (20). The low activation energies for the catalyzed C–N_2O reaction are a strong indication that the dissociation of N_2O can form a very abundant amount of epoxy oxygen intermediate. The relative activities of different catalysts depend on two factors: (1) The activity of the catalyst to dissociate the reactant molecule to form O atoms, which in turn form the epoxy oxygen intermediate; (2) the extent of the C–C bond weakening by the metal (*M*) or by the adjacent phenolate (–C–O–*M*) groups (8).

ACKNOWLEDGMENTS

Financial support from the Department of Education, Commonwealth Government of Australia and also the U.S. National Science Foundation is gratefully acknowledged.

REFERENCES

1. Kapteijn, F., Alexander, J. C., Mierop, G. A., and Moulijn, J. A., *J. Chem. Soc. Chem. Commun.* 1084 (1984).
2. Verra, M. J., and Bell, A. T., *Fuel* **57**, 194 (1978).
3. Kapteijn, F., Abbel, G., and Moulijn, J. A., *Fuel* **63**, 1036 (1984).
4. Kapteijn, F., Peer, O., and Moulijn, J. A., *Fuel* **65**, 1371 (1986).
5. Okuhara, T., and Tanaka, K., *J. Chem. Soc. Faraday Trans.* **82**, 3657 (1986).
6. Illán-Gómez, M. J., Linares-Solano, A., Radovic, L. R., and Salinas-Martínez de Lecea, C., *Energy Fuels* **9**, 97 (1995).
7. Illán-Gómez, M. J., Linares-Solano, A., Radovic, L. R., and Salinas-Martínez de Lecea, C., *Energy Fuels* **9**, 104 (1995).
8. Huang, H. Y., and Yang, R. T., *J. Catal.* **185**, 286 (1999).
9. Ruckenstein, E., and Hu, Y. H., *Ind. Eng. Chem. Res.* **36**, 2533 (1997).
10. Yamashita, H., Tomita, A., Yamada, H., Kyotani, T., and Radovic, L. R., *Energy Fuels* **7**, 85 (1993).
11. Li, Y. H., Lu, G. Q., and Rudolph, V., *Chem. Eng. Sci.* **53**, 1 (1998).
12. Aarna, I., and Suuberg, E. M., *Fuel* **76**, 475 (1997).
13. Illán-Gómez, M. J., Linares-Solano, A., Radovic, L. R., and Salinas-Martínez de Lecea, C., *Energy Fuels* **10**, 158 (1996).
14. Pels, J. R., Ph.D. Thesis, Delft University of Technology, Delft, The Netherlands, 1995.
15. Zhu, Z. H., and Lu, G. Q., *J. Catal.* **187**, 262 (1999).
16. Walker, P. L., Jr., Rusinko, F., Jr., and Austin, L. G., *in* "Advances in Catalysis" (D. D. Eley, P. W. Selwood, and P. B. Weisz, Eds.), Vol. 11, p. 133. Academic Press, New York, 1959.
17. McKee, D. W., *in* "Chemistry and Physics of Carbon" (P. L. Walker, Jr., and P. A. Thrower, Eds.), Vol. 16. Dekker, New York, 1980.
18. McKee, D. W., and Chatterji, S., *Carbon* **20**, 59 (1982).
19. Chen, S. G., and Yang, R. T., *Energy Fuels* **11**, 421 (1997).
20. Chen, N., and Yang, R. T., *J. Phys. Chem. A* **102**, 6348 (1998).
21. Petrakis, D. E., Pomonis, P. J., and Sdoukos, A. T., *J. Chem. Soc. Faraday Trans. 1* **85,** 3173 (1989).
22. Zielinski, J., *Appl. Catal.* **35**, 1 (1987).
23. Pomonis, P., Vattis, D., Lycourghiotis, A., and Kordulis, C., *J. Chem. Soc. Faraday Trans. 1* **81**, 2043 (1985).
24. Bartley, G. J., Burch, R., and Chappell, J., *Appl. Catal.* **43**, 91 (1988).
25. Evans, J. W., Wainwright, M. S., Bridgewater, A. J., and Young, D. J., *Appl. Catal.* **7**, 75 (1983).
26. Zhu, Z. H., Radovic, L. R., and Lu, G. Q., *Carbon*, **38**, 451 (2000).
27. Lang, R. L., *Fuel* **65**, 1324 (1986).
28. Cerfontain, M. B., Meijer, R., Kapteijn, F., and Moulijn, J. A., *J. Catal.* **107**, 173 (1987).
29. Meijer, R., Weeda, M., Kapteijn, F., and Moulijn, J. A., *Carbon* **29**, 929 (1991).
30. Kodama, C., Orita, H., and Nozoye, H., *Appl. Surf. Sci.* **121/122**, 579 (1997).
31. De Rossi, S., Ferraris, G., and Mancini, R., *Appl. Catal.* **38**, 359 (1988).
32. Rodriguez-Reinoso, F., Garrido, J., Martin-Martinez, J. M., Molina-Sabio, M., and Torreogrosa, R., *Carbon* **27**, 23 (1989).
33. Garrido, J., Linares-Solano, A., Martin-Martinez, J. M., and Rodriguez-Reinoso, F., *Langmuir* **3**, 76 (1987).
34. Ratcliffe, C. T., and Vaughn, S. N., *ACS Prepr. Div. Fuel Chem.* **30**, 304 (1985).
35. Linares-Solano, A., Almela-Alarcón, M., and Salinas-Martí nez de Lecea, C., *J. Catal.* **125**, 401 (1990).
36. Hippo, E. J., Jenkins, R. G., and Walker, P. L., Jr., *Fuel* **65**, 776 (1979).
37. Linares-Solano, A., Salinas-Martínez de Lecea, C., Caporla-Amorós, D., Joly, J. P., and Charcosset, H., *Energy Fuels* **4**, 467 (1990).
38. Mims, C. A., and Pabst, J. K., *J. Catal.* **107**, 209 (1987).
39. Pan, Z. J., and Yang, R. T., *Ind. Eng. Chem. Res.* **31**, 2675 (1992).
40. Chen, S. G., and Yang, R. T., *J. Catal.* **138**, 12 (1992).
41. Chen, S. G., Yang, R. T., Kapteijn, F., and Moulijn, J. A., *Ind. Eng. Chem. Res.* **32**, 2835 (1993).
42. Chen, S. G., and Yang, R. T., *J. Catal.* **141**, 102 (1993).
43. Chang, J. S., Lauderback, L. L., and Falconer, J. L. *Carbon* **29**, 645 (1991).
44. Richthofen, A. V., Wendel, E., and Neuschutz, *Fresenius J. Anal. Chem.* **346**, 261 (1993).
45. Pauling, L., "The Nature of the Chemical Bond." Cornell University Press, Ithaca, NY, 1960.
46. Brodén, G., Rhodin, T. N., and Brucker, C., *Surf. Sci.* **59**, 593 (1976).
47. Winter, E. R. S., *J. Catal.* **34**, 431 (1974).
48. Li, Y., and Armor, J. N., *Appl. Catal. B* **1**, L31 (1992).
49. Yamashita, T., and Vannice, M. A., *J. Catal.* **161**, 254 (1996).
50. Teng, H., Lin, H., and Hsieh, Y., *Ind. Eng. Chem. Res.* **36**, 523 (1997).